

Dispersal probability distributions and the wave-front speed problem

Vicenç Méndez,¹ Toni Pujol,² and Joaquim Fort^{2,*}

¹*Facultat de Ciències de la Salut, Universitat Internacional de Catalunya, c/ Gomera s/n, 08190-Sant Cugat del Vallès, Barcelona, Spain*

²*Departament de Física, Universitat de Girona, Campus Montilivi, 17071 Girona, Catalonia, Spain*

(Received 28 December 2001; published 10 April 2002)

The speed and width of front solutions to reaction-dispersal models are analyzed both analytically and numerically. We perform our analysis for Laplace and Gaussian distribution kernels, both for delayed and nondelayed models. The results are discussed in terms of the characteristic parameters of the models.

DOI: 10.1103/PhysRevE.65.041109

PACS number(s): 05.40.Jc, 05.60.-k, 82.20.-w

I. INTRODUCTION

Reaction-diffusion models have been widely used to describe a large number of physical, chemical, and biological problems when dispersal is coupled to reaction [1]. The prototype is Fisher's equation $\partial_t \rho = \partial_{xx} \rho + f(\rho)$ where $\rho > 0$, f is a nonlinear function of ρ and typically $f(0) = f(1) = 0$. As shown rigorously by Aronson and Weinberger [2], for a sufficiently localized initial condition the solution to this equation evolves into a wave front which connects the homogeneous steady states $\rho = 1$ (stable) to $\rho = 0$ (unstable) traveling with the minimal possible speed. Another important approach is able to model more general dispersal processes than diffusive ones, as well as long-range effects. In this framework, one resorts to integrodifferential or integrodifference equations. Let us denote such approaches under the name reaction-dispersal models [3]. Their differences with respect to the reaction-diffusion approach will be made clear below. Mathematically, the later makes use of differential, as opposed to integrodifferential or integrodifference, evolution equations. Reaction-dispersal models are based on considering a kernel probability distribution, which quantifies the probability of dispersing as a function of distance. For models that describe the spread of invading organisms often one assumes that the kernel is Gaussian, but in practice it should be estimated from observed data [4].

It is important to stress that many reaction-dispersion systems do not exhibit wave-front solutions. Accordingly, here we shall here consider a specific class of systems for which this behavior does arise, namely, those in which the system has two equilibrium states, one of them being stable and the other one unstable. Moreover, the dispersion will be described by means of a kernel, in contrast to the more usual, diffusive approach in which it is described as a Laplacian of the particle number density in the particle number evolution equation (this classical limit will be retrieved as a special case). Also, the initial condition we shall use is such that all particles are initially confined to a finite region, since it is known from the diffusive (i.e., classical) limit that for non-compact initial conditions the solution may in general be different from a wave front [2].

In this paper, we study the wave-front speed problem for reaction-dispersal systems that have been applied to ecologi-

cal problems [3,5,6], biological invasions [7], human-mediated dispersal [8], and in general, to spatial spread phenomena with long-range interaction [1]. Our main motivation is that analytical formulas for the speed and width of fronts have not been previously derived for such cases, in spite of their practical importance. We make use of marginal stability analysis for fronts traveling into an unstable state [9], a method developed originally for reaction-diffusion equations. This analysis is extended here to reaction-dispersal equations, and compared to numerical solutions, to determine the speed and also the width of emerging fronts. Our models are based in a dispersal probability distribution given by Gaussian (normal) or Laplace (leptokurtic) kernels. Our interest is to observe the effect of the underlying random walk (through the specific kernel) and of the characteristic waiting time τ between successive jumps on the front velocity. Finally we also study, again both analytically and numerically, the effect of these parameters on the width of the front.

II. REACTION-DISPERSAL MODELS

Let $\rho(x, t)$ be the density of particles in x at time t . We assume that all the particles wait a time τ between two successive jumps. After a time τ the density of particles is given by two contributions: on one hand, the density of particles which jump to x at the time $t + \tau$, and on the other hand, the particle created from a nonlinear source term $F(\rho) = rf(\rho)$ where r is the characteristic rate of reproduction. Then one writes the following integrodifference equation:

Model A:

$$\rho(x, t + \tau) = \int_{-\infty}^{\infty} \rho(x + \Delta, t) \varphi(\Delta) d\Delta + \tau r f(\rho), \quad (1)$$

where the kernel $\varphi(\Delta)$ means the probability distribution function of jumps length, so that $\varphi(\Delta)$ yields the probability that a particle makes a jump of length Δ (Δ may be positive or negative). Consider isotropic kernels [i.e., $\varphi(\Delta) = \varphi(-\Delta)$]. The moments of the kernel are given by

$$\langle \Delta^n \rangle \equiv \int_{-\infty}^{\infty} \Delta^n \varphi(\Delta) d\Delta, \quad (2)$$

*Email address: joaquim.fort@udg.es

where $\langle \Delta^n \rangle = 0$ for odd n . On the other hand, the normalization condition reads $\langle \Delta^0 \rangle = 1$. The integral in Eq. (1) must be done over the set of possible lengths of jump Δ . Model A has been already studied in order to find out the possible speeds of wave fronts by applying Hamilton-Jacobi theory for a specific kernel [10] in which all particles jump the same distance. That kernel, which is different from those considered by us below, is very interesting conceptually but not very realistic from a practical point of view [11,12].

The continuous version for Model A (i.e., Fedotov's Model B [10]) is nothing but the first-order expansion of the left-hand side of Eq. (1) for $\tau \ll t$. In this way, one gets the following nondelayed integrodifferential equation:

Model B:

$$\partial_t \rho(x, t) = \lambda \left[\int_{-\infty}^{\infty} \rho(x + \Delta, t) \varphi(\Delta) dz - \rho(x, t) \right] + r f(\rho), \quad (3)$$

where $\lambda = 1/\tau$. Both Models A and B shall be considered in this paper.

A. Limiting cases

By expanding the terms $\rho(x, t + \tau)$ and $\rho(x + \Delta, t)$ in Eq. (1) in Taylor series for $\tau \ll t$ and $\Delta \ll x$ one has, in general

$$\sum_{n=1}^{\infty} \frac{\tau^n}{n!} \partial_t^n \rho(x, t) = \sum_{n=1}^{\infty} \frac{\langle \Delta^{2n} \rangle}{(2n)!} \partial_x^{2n} \rho(x, t) + \tau r f(\rho). \quad (4)$$

Up to the first order in τ and up to second order in Δ , this yields the following equation:

$$\partial_t \rho = D \partial_{xx} \rho + r f(\rho), \quad (5)$$

which is the well-known Fisher–Kolmogorov–Petrovskii–Piskunov equation, and $D \equiv \langle \Delta^2 \rangle / (2\tau)$ is the diffusion coefficient, given in terms of the second moment of the distribution function $\varphi(\Delta)$.

On the other hand, up to the second order in τ and up to second order in Δ , the following equation is obtained:

$$\frac{\tau}{2} \partial_{tt} \rho + \partial_t \rho = D \partial_{xx} \rho + r f(\rho). \quad (6)$$

This equation has been recently studied to take into account memory effects in the transport process [13].

III. FRONT SPEED PROBLEM

To study the front speed problem, we will make use of the marginal stability analysis to find the speed of wave fronts in terms of a dispersal relation $\omega = \omega(k)$ where, in principle, ω and k may be complex numbers. Once the dispersal relation is obtained, the asymptotic speed v^* is given by $v^* = \omega^*/k^*$ where $\omega^* = \omega(k^*)$, $k^* = ik_i^*$, $k_r^* = 0$, $\omega^* = i\omega_i^*$, and $\omega_r^* = 0$. The subscripts i and r indicate the imaginary and real parts, respectively. The value of k_i^* must be computed from the condition $\omega_i^*/k_i^* = d\omega_i^*/dk_i^*$ [14]. This condition,

however, is equivalent to demand that the speed must have a minimum at k_i^* , that is $dv^*/dk_i^* = 0$ as may be easily checked.

The growth term $f(\rho)$ we use in this paper is such that $f(0) = f(1) = 0$ where $\rho = 1$ and $\rho = 0$ are the homogeneous steady states, stable and unstable, respectively, and $f'(0) > 0$. A specific case which will be used for numerical simulations is the logistic growth $f(\rho) = \rho(1 - \rho)$.

A. Speed of fronts in Model A

We show now how to derive the speed of wave fronts traveling into the unstable state $\rho = 0$, for systems evolving according to Eq. (1) by linearizing $f(\rho)$ around the unstable state $\rho = 0$, that is, $f(\rho) \approx f'(0)\rho$. Then

$$\rho(x, t + \tau) = \int_{-\infty}^{\infty} \rho(x + \Delta, t) \varphi(\Delta) d\Delta + \beta \rho, \quad (7)$$

where

$$\beta \equiv r \tau f'(0).$$

We propose a plane traveling wave solution with the form $\rho(x, t) \sim \exp[i(kx - \omega t)]$ which introduced into Eq. (7) yields the dispersion relation

$$e^{-i\omega\tau} = \tilde{\varphi}(k) + \beta, \quad (8)$$

where

$$\tilde{\varphi}(k) \equiv \int_{-\infty}^{\infty} e^{ik\Delta} \varphi(\Delta) d\Delta = \sqrt{2\pi} \mathcal{F}[\varphi(k)], \quad (9)$$

and $\mathcal{F}[\varphi(k)]$ is the Fourier transform of the kernel. The dispersal relation is given, from Eq. (8), by

$$\omega = \frac{-1}{i\tau} \ln[\tilde{\varphi}(k) + \beta],$$

and the asymptotic speed is

$$v^* = \frac{\omega(k = ik_i^*)}{ik_i^*} = \min_{k_i^*} \left\{ \frac{1}{\tau k_i^*} \ln[\hat{\varphi}(k_i^*) + \beta] \right\}, \quad (10)$$

where $\hat{\varphi}(k_i^*) \equiv \tilde{\varphi}(ik_i^*)$. In order to find out the minimum speed we must find the value of k_i^* such that the relation $dv^*/dk_i^* = 0$ is fulfilled. Taking into account Eq. (10), k_i^* must be found from

$$[\hat{\varphi}(k_i^*) + \beta] \ln[\hat{\varphi}(k_i^*) + \beta] = k_i^* \frac{d\hat{\varphi}(k_i^*)}{dk_i^*}, \quad (11)$$

which lead us to a transcendental equation for k_i^* . However, we can find approximate analytical solutions. Let us now to consider two specific random walks described by typical probability distribution functions of jumps. The delta kernel used in Ref. [10] assumes that all particles jump the same length. However, both in physical and in biological pro-

cesses, this is known to be a rather extreme approximation to the observed dispersal distance distributions [4,11,12]. Therefore, we apply the above analysis to dispersal kernels that have been often used in the literature, although their corresponding front speeds have not been previously obtained.

The most usual kernel is the so-called normal or Gaussian one, namely,

$$\varphi(\Delta) = \frac{1}{\alpha\sqrt{\pi}} e^{-\Delta^2/\alpha^2}.$$

For this kernel, $\tilde{\varphi}(k) = \exp(-k^2\alpha^2/4)$, $\hat{\varphi}(k_i^*) = \exp(k_i^{*2}\alpha^2/4)$ and $\langle \Delta^n \rangle = \alpha^n \Gamma(n+1/2)/\sqrt{\pi}$ for even n and 0 for odd n . The kurtosis of the kernel,

$$B_2 = \frac{\langle \Delta^4 \rangle}{(\langle \Delta^2 \rangle)^2}$$

is a measure of the disparity of spatial scales for the dispersal process. Leptokurtic kernels have $B_2 > 3$, and the Gaussian kernel has $B_2 = 3$, as may be easily checked.

We assume that the minimum is attained for $k_i^* \alpha < 1$, so that we expand Eq. (11) up to second order in $k_i^* \alpha$ and we find

$$k_i^* \approx \frac{2}{\alpha} \left[\frac{(1+\beta)\ln(1+\beta)}{1+\beta\ln(1+\beta)} \right]^{1/2}.$$

Finally, the minimum speed is, from Eq. (10), given by

$$v^* \approx \frac{\alpha}{2\tau} \left[\frac{1+\beta\ln(1+\beta)}{(1+\beta)\ln(1+\beta)} \right]^{1/2} \times \ln[(1+\beta)^{(1+\beta)/(1+\beta\ln(1+\beta))} + \beta]. \quad (12)$$

The second kernel we use is the Laplace kernel [11,15]

$$\varphi(\Delta) = \frac{1}{2\alpha} e^{-|\Delta|/\alpha}.$$

For this kernel, $\tilde{\varphi}(k) = 1/(1+k^2\alpha^2)$, $\hat{\varphi}(k_i^*) = 1/(1-k_i^{*2}\alpha^2)$ and $\langle \Delta^n \rangle = \alpha^n n!$ for even n and 0 for odd n . The kurtosis of this kernel is $B_2 = 6 > 3$, i.e., it is leptokurtic. These kinds of kernels have been found more realistic for ecological problems than the Gaussian ones [11]. In this case, the minimum value for the speed of the front must be computed within the interval $k_i^* \in (0, 1/\alpha)$ to guarantee the positive and finite value for $\hat{\varphi}(k_i^*)$, so that in this case we also consider $k_i^* \alpha < 1$. Expanding Eq. (11) up to second order in $k_i^* \alpha$ and we get

$$k_i^* \approx \frac{1}{\alpha} \left[\frac{(1+\beta)\ln(1+\beta)}{1+(1+2\beta)\ln(1+\beta)} \right]^{1/2},$$

and the speed at this point is found to be

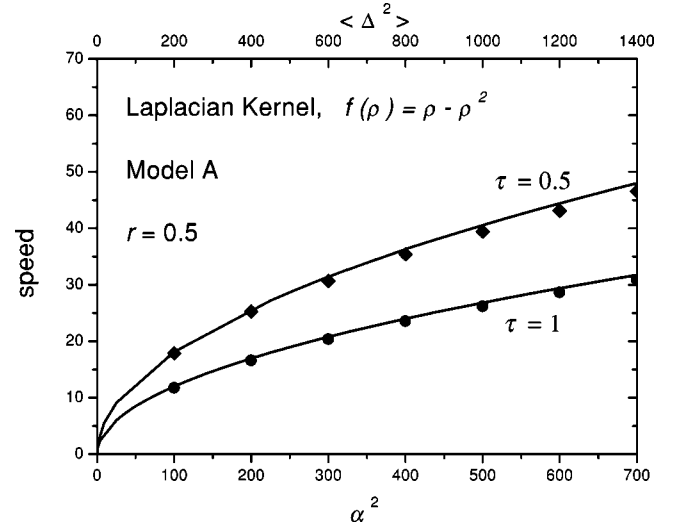


FIG. 1. Comparison between numerical (symbols) and analytical [solid lines obtained from Eq. (13)] solutions for the speed of fronts in Model A for Laplacian dispersion. We have used $r=1/2$ and a logistic reaction term $f(\rho) = \rho(1-\rho)$. The speed of the front for $\tau=1$ is lower than for $\tau=0.5$.

$$v^* \approx \frac{\alpha}{\tau} \left[\frac{1+(1+2\beta)\ln(1+\beta)}{(1+\beta)\ln(1+\beta)} \right]^{1/2} \times \ln \left[\frac{1+\beta+(1+\beta)^2\ln(1+\beta)}{1+\beta\ln(1+\beta)} \right]. \quad (13)$$

The analytical solutions obtained for both kernels have been compared to the numerical solutions to the transcendental Eq. (11), and also to the speed of fronts observed in numerical simulations of Eq. (1). We have performed the numerical simulations by using a logistic growth term [$f(\rho) = \rho(1-\rho)$] and a “double-step” function for the initial profile, namely,

$$\rho(x,t=0) = \begin{cases} 0 & \text{if } x < -x_0 \\ 1 & \text{if } -x_0 < x < x_0, \\ 0 & \text{if } x > x_0 \end{cases} \quad (14)$$

and applying the fast-Fourier-transform (FFT) method, which allows us to derive precise results in a much shorter computer time [16].

In Figs. 1 and 2 we plot the speeds observed in the numerical simulations for Model A (symbols), as well as the analytical predictions (solid lines), for Laplacian (Fig. 1) and Gaussian (Fig. 2) dispersal. We have checked that the predictions of the transcendental Eq. (11) are the same as those of the explicit analytical Eqs. (12) and (13) [full curves in Figs. 1 and 2]. We observe that in Figs. 1 and 2, Eqs. (12) and (13) are very good approximations since they agree with the simulations, and we note that the speed increases with the characteristic dispersal distance α , as was to be expected intuitively. In both figures one observes that the speed is lower for higher values of the waiting time τ , also as expected. From Eqs. (12) and (13) we obtain that the speed varies linearly with α . However, in Figs. 1 and 2, as well as

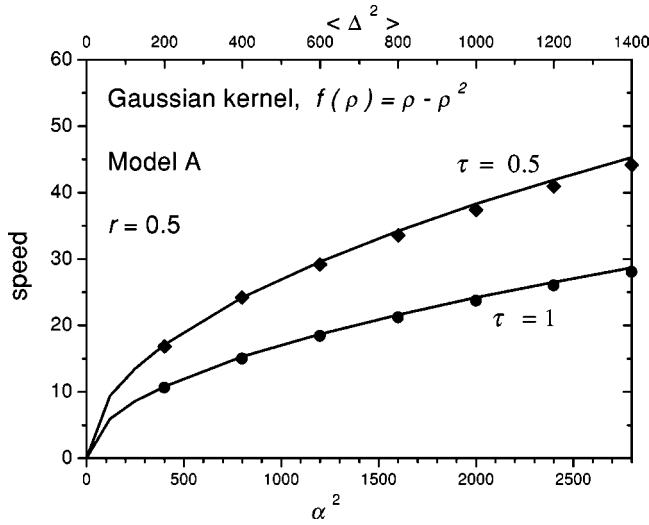


FIG. 2. Comparison between numerical (symbols) and analytical [solid lines obtained from Eq. (12)] solutions for the speed of fronts in Model A for Gaussian dispersion. We have taken $r=1/2$ and a logistic reaction term $f(\rho)=\rho(1-\rho)$.

in Fig. 3 for Model B, we use α^2 (and $\langle \Delta^2 \rangle$, which is proportional to α^2) rather than α as independent variable, because α , in contrast to the mean-square jump distance $\langle \Delta^2 \rangle$, does not have a single physical interpretation for both kernels. Note that for the Laplacian kernel $\langle \Delta^2 \rangle = 2\alpha^2$, whereas for the Gaussian one $\langle \Delta^2 \rangle = \alpha^2/2$. Comparing Figs. 1 and 2, we also see that the Laplace kernel gives a higher front speed. This could have been expected intuitively because the Gaussian kernel decays faster with distance, so that fewer particles disperse to high distances. We can expect then, in general, that the speed of fronts increases with the kurtosis of the kernel and therefore leptokurtic kernels yield higher speed of front than platikurtic ($B_2 < 3$) kernels. Although a general proof is not available, we have noted that this is

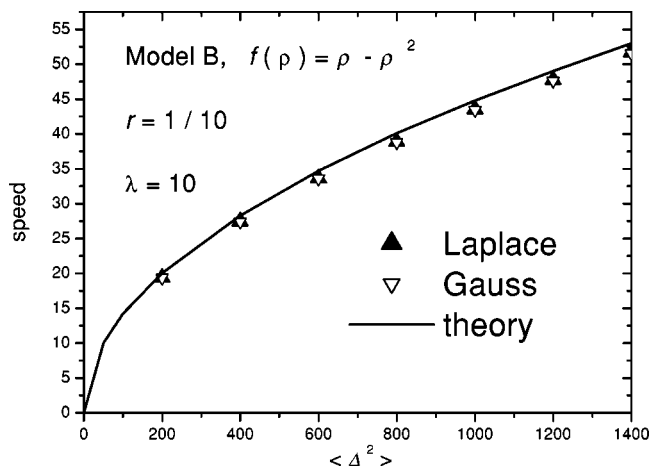


FIG. 3. Comparison between numerical (symbols) and analytical [solid curve, $v^* \approx 2\sqrt{\langle \Delta^2 \rangle}/2\sqrt{\gamma\lambda}$ from Eq. (21)] solutions for the speed of fronts in Model B. The speed of the fronts for Laplacian and Gaussian kernels is the same since $r/\lambda \ll 1$. We have used $r=1/10$, $\lambda=10$, and a logistic reaction source function $f(\rho)=\rho(1-\rho)$.

consistent with physical intuition and our analytical and numerical results.

B. Speed of fronts in model B

We also linearize Eq. (3) around the unstable state $\rho=0$, so that

$$\partial_t \rho(x,t) = \lambda \left[\int_{-\infty}^{\infty} \rho(x+\Delta,t) \varphi(\Delta) dz - \rho(x,t) \right] + \gamma \rho, \quad (15)$$

where $\gamma = rf'(0)$. Assuming a plane traveling wave, we have the dispersal relation

$$-i\omega = \lambda [\tilde{\varphi}(k) - 1] + \gamma, \quad (16)$$

where $\tilde{\varphi}(k)$ is given by Eq. (9). The asymptotic speed is given then by

$$v^* = \frac{\omega(k=ik_i^*)}{ik_i^*} = \min \left\{ \frac{\lambda [\hat{\varphi}(k_i^*) - 1] + \gamma}{k_i^*} \right\}. \quad (17)$$

We must find now the value of k_i^* such that the relation $dv^*/dk_i^* = 0$ is fulfilled. Taking into account Eq. (17), k_i^* must be found from

$$\hat{\varphi}(k_i^*) + \frac{\gamma}{\lambda} - 1 = k_i^* \frac{d\hat{\varphi}(k_i^*)}{dk_i^*}. \quad (18)$$

For the Gaussian kernel, we assume that the minimum is attained for $k_i^* \alpha < 1$. If one expands Eq. (18) up to second order in $k_i^* \alpha$ one gets

$$k_i^* \alpha \approx 2\sqrt{\gamma/\lambda},$$

and from Eq. (17) one obtains

$$v^* \approx \frac{\alpha}{2} \sqrt{\frac{\lambda}{\gamma}} (\lambda e^{\gamma/\lambda} - \lambda + \gamma). \quad (19)$$

For the Laplace kernel, one proceeds along the same way and the value for k_i^* which minimizes the speed is given by

$$k_i^* \alpha \approx \sqrt{\frac{\gamma/\lambda}{1+2\gamma/\lambda}},$$

and the speed is given by

$$v^* \approx \alpha \frac{2\lambda + \gamma}{\lambda + \gamma} \sqrt{\gamma\lambda + 2\gamma^2}. \quad (20)$$

Let us now assume that $\gamma = rf'(0) \ll \lambda$. The physical meaning of this approximation is the following: since λ^{-1} and r^{-1} are the timescales of the dispersal and reactive processes, respectively, for a logistic growth with $f'(0)=1$ the limit $r \ll \lambda$ holds when dispersal process is much faster (or

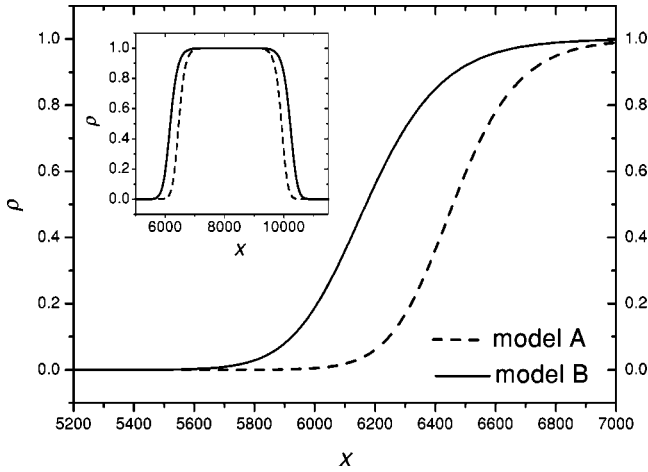


FIG. 4. Front profiles for $r=0.1$ and the Laplacian kernel with $\alpha^2=700$. In Model B $\lambda=1/\tau$, with $\tau=2$ the value used in Model A, as explained in the main text. Note that Model B yields a faster front, which also has a wider reaction zone.

equivalently, the delay time τ is low enough) than the growth process. In this case, it is interesting to note that both Eqs. (19) and (20) yield

$$v^* \approx 2\sqrt{\langle \Delta^2 \rangle} / 2\sqrt{\gamma\lambda} = 2\sqrt{Dr}, \quad (21)$$

where the diffusion coefficient is given by $D = \langle \Delta^2 \rangle / (2\tau)$ and $\lambda = \tau^{-1}$. Note that this additional approximation $r\tau \ll 1$ does not hold for cases such as those in Figs. 1 and 2. Therefore, in Fig. 3 we check the agreement between both Models A and B for $r\tau = 0.01 \ll 1$. Both the simulation and the theoretical results yield the same speeds, as expected, because Model B reduces to Model A if $\lambda = 1/\tau$ and $\tau \ll 1/r$ holds. The physical reason for this agreement is that the effect of the delay time is small enough so that Fisher's approach [Eq. (5), which neglects the role of the term in τ appearing in Eq. (6)] holds approximately. However, we stress that if the approximation $r\tau \ll 1$ breaks down, then Models A and B yield different results. This may be seen in Figs. 4 and 5 (e.g., $r\tau = 0.2$ in Fig. 4), where the predictions of both models are seen to be very different, as checked by the numerical simulations. It shows that Model B, which is only a first-order approximation to Model A, is not available to capture the detailed dynamics of the front. Therefore, when dealing with specific applications, in order to distinguish clearly the consequences of the dispersion probability kernel on the front speed, Model A should be preferred to Model B, unless there is some experimental information relative to the microscopic random-walk rest time probability distribution function (see Refs. [10,17,18]).

Figure 4 presents some simulated fronts according to both models. It is seen that Model B, which is only an approximation to Model A, yields a faster front (Fig. 4, inset). It is also seen that Model B yields a wider front (main Fig. 4). This is also shown in Fig. 5, for several values of the delay time τ , and is discussed in more detail in Sec. IV below.

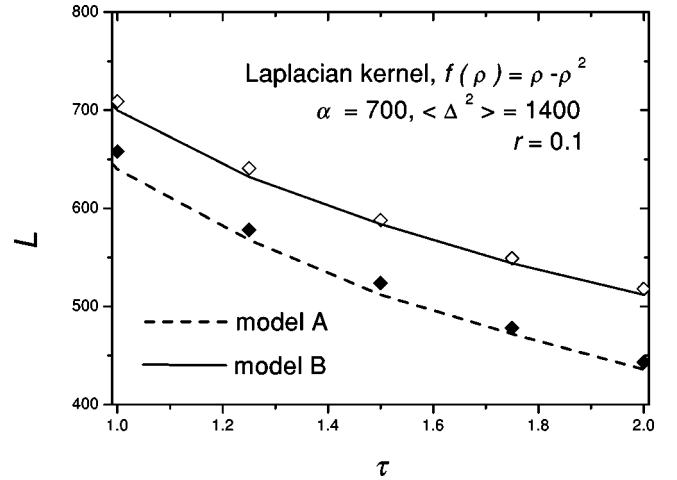


FIG. 5. Front width versus delay time. The rhombs are the results from the numerical simulations, and the curves are the theoretical predictions. In Model B, $\lambda = 1/\tau$ so that Model B is a first-order approximation to the full dynamics described by Model A. The front speed is proportional to the front width L [see Eq. (23)].

IV. WIDTH OF WAVE FRONT

The knowledge of the width of a front is interesting in virus phage fronts, where the front profile may be observed directly in order to validate models [19], as well as in the context of fire fronts, where the width of the combustion zone is a relevant prediction [20]. From Fig. 4 we observe that there exists an inflection point x^* such that $\partial_x \rho$ reaches a maximum value at $x = x^*$ and $(\partial_x^{2n} \rho)_{x=x^*} = 0$ for $n = 1, 2, 3, \dots$. In the limit $\tau \ll t$ one has from Eqs. (1) and (4)

$$\begin{aligned} \rho(x^*, t + \tau) &\approx \rho(x^*, t) + \tau \partial_t \rho|_{x=x^*} \\ &= r\tau f(\rho)|_{x=x^*} + \rho(x^*, t), \end{aligned}$$

so that

$$\tau \partial_t \rho|_{x=x^*} \approx r\tau f(\rho)|_{x=x^*}. \quad (22)$$

We change into a frame moving with the front by defining the coordinate $z \equiv x - v^*t$. For $x = x^*$ one has $z^* \equiv x^* - v^*t$ and from Eq. (22) we get $-v^* \partial_z \rho|_{z=z^*} \approx r f(\rho)|_{x=x^*}$. The width of the front L is given by

$$L^{-1} = -\partial_z \rho|_{z=z^*} \approx \frac{r}{v^*} f(\rho)|_{z=z^*}. \quad (23)$$

In Fig. 5 we compare this prediction to the results of numerical simulations for a logistic reactive process $[f(\rho)|_{z=z^*} = f(\frac{1}{2}) = \frac{1}{4}]$. The front width is estimated from the simulated profiles by fitting a straight line to the central range ($\rho \approx 1/2$) of profiles such as those in Fig. 4 and, as mentioned above, the front width is estimated as the inverse of the slope of the fitted line. From Fig. 5, we see that there is good agreement with the theoretical prediction given by Eq. (23). Note that from Eq. (23), the front speed is proportional to the front width in both models. A higher value of the delay time corresponds to a narrower, slower front, as was to

be expected. Figure 5 shows that, the higher the value of τ , the more error results from using Model B as an approximation to Model A, also as expected. This error is higher than 20% in Fig. 5 and is the same for the front speed and the front width, because they are proportional to each other [see Eq. (23), which makes it possible to determine the speed from any value of the front width in Fig. 5]. Therefore, when using Model B as an approximation to Model A, one should previously see if the error, computed in the way explained in this paper and illustrated by Fig. 5, is negligible or not for the parameter values used.

V. CONCLUSIONS

We have studied the speed of fronts for integrodifference (Model A) and integrodifferential (Model B) equations that model reaction-dispersal processes. These models have been applied to a wide range of ecological invasions [3,6,11]. In the present paper, the dispersal process has been modeled by Laplace and Gaussian kernels, and all of the particles wait a time τ below making the next jump. When dispersal and reaction work together, traveling wave fronts can appear. The asymptotic speed of the fronts, which was previously un-

known, has been derived from the marginal stability analysis usually employed for reaction-diffusion processes [9]. Approximate analytical expressions for the speed have been found and compared with numerical simulations, exhibiting rather good agreement. We have shown how the speed diminishes with increasing values of the waiting time τ , and increases with the characteristic length of jump α . The Laplace kernel yields a higher front speed than the Gaussian one, which exhibits that leptokurtic kernels should be expected intuitively to yield higher front speeds than platikurtic ones. When the waiting time τ is small ($t \gg \tau$), Model A may be approximated by Model B. For $\tau \ll r^{-1}$, one recovers Fisher's result from both models. However, in general, Model B yields a faster, as well as wider, front than Model A—again in agreement with our theoretical formulas.

ACKNOWLEDGMENTS

The computing equipment used was funded in part by the CICYT of the Ministry of Science and Technology under Grant Nos. BFM 2000-0351 and SGR-2001-00186 (V.M. and J.F.) and REN 2000-1621 CLI (T.P. and J.F.).

-
- [1] J. Murray, *Mathematical Biology* (Springer-Verlag, New York, 1989).
- [2] D.G. Aronson and H.F. Weinberger, *Adv. Math.* **30**, 33 (1978).
- [3] M. Kot, *J. Math. Biol.* **30**, 413 (1992).
- [4] B. W. Silverman, *Density Estimation for Statistics and Data Analysis* (Chapman and Hall, London, 1986).
- [5] A. Hastings and K. Higgins, *Science* **263**, 1133 (1994).
- [6] M.G. Neubert, M. Kot, and M.A. Lewis, *Theor. Popul. Biol.* **48**, 7 (1995).
- [7] F. van den Bosch, R. Hengeveld, and J.A.J. Metz, *J. Biogeogr.* **19**, 135 (1992).
- [8] A.V. Suárez, D.A. Holway, and T.J. Case, *Proc. Natl. Acad. Sci. USA* **98**, 1095 (2001).
- [9] U. Ebert and W. van Saarloos, *Physica D* **146**, 1 (2000).
- [10] S. Fedotov, *Phys. Rev. Lett.* **86**, 926 (2001).
- [11] M. Kot, M.A. Lewis, and P. van den Driessche, *Ecology* **77**, 2027 (1996).
- [12] R.R. Veit and M.A. Lewis, *Am. Nat.* **148**, 255 (1996).
- [13] K.K. Manne, A.J. Hurd, and V.M. Kenkre, *Phys. Rev. E* **61**, 4177 (2000).
- [14] Note that the condition of minimum speed $\omega_i^*/k_i^* = d\omega_i^*/dk_i^*$ is equivalent to the condition (16) given in Ref. [10].
- [15] R.A.J. Taylor, *Ecol. Entomol.* **3**, 63 (1978).
- [16] W. H. Press, S. A. Teukolsky, W. T. Vetterling, and B. P. Flannery, *Numerical Recipes in Fortran 77. The Art of Scientific Computing*, 2nd ed. (Cambridge University Press, Cambridge, England, 1996).
- [17] V. Méndez and J. Camacho, *Phys. Rev. E* **55**, 6476 (1997).
- [18] J. Fort and V. Méndez, *Phys. Rev. Lett.* **82**, 867 (1999).
- [19] J. Yin, *Biochem. Biophys. Res. Commun.* **174**, 1009 (1991).
- [20] V. Méndez and J.E. Lleboto, *Phys. Rev. E* **56**, 6557 (1997).